

Review: Applications, Compositions, and Performances of Lithium Ion Batteries in Electric Vehicles

Rawand S. Abdullah, Mazin A. Othman and Rostam R. Braiem

Department of Chemistry, College of Science, Salahaddin University-Erbil, Erbil, Kurdistan Region, Iraq

Abstract—The most of air pollution from our region is due to gases emission from traditional vehicles. To solve this, electric vehicles (EVs) are the best choice. EVs work by lithium-ion battery (LIB). In this review, we focused on the recent invented LIBs, their compositions and their performances in EVs. Then, it indicates these compartments compositions (electrolytic solution and electrodes) are more suitable and portable with its best performance in the application for EVs. Finally, it discusses the methods and mechanism of recharging and discharging of the LIBs.

Index Terms—Capacity, Composition, Electric vehicles, Electrolyte, Electrode, Lithium-ion.

I. INTRODUCTION

The recent advances in the lithium-ion battery (LIB) concept toward the development of sustainable energy storage systems are presented. The study reports on new Li-ion cells developed over the past few years with the aim of improving the performance and sustainability of electrochemical energy storage [1]. Li is one of the lightest elements with high reactive and electrochemical potential which makes it an ideal material for a battery. Li-ion is used instead of metallic Li. Thus, LIB is able to achieve high energy density, good life cycle, higher cell voltage, easier maintenance, and environmentally friendly compared with other types of batteries [2]. Therefore, the Li became the logical choice to replace lead as it is the lightest metal available in the world. Li ion is manufactured from Li salts which are extracted from mining activities. Nowadays, LIBs are used in almost all gadgets including laptop, cell phone, camera, iPod, and many more devices and hence they are very popular these days [3]. Consequently, global demand for electric vehicles (EVs) has exploded in recent years.

More than 740,000 EVs were on the road in January 2015, a number expected to reach several million by 2020. LIBs will be power all of the electric cars [4]. In addition, for maximum performance, all of the large packs of series connected Li ion cells require a battery management system that must provide several functions [5].

Environmental problems triggered by emissions from conventional vehicles have accelerated the adaptation of EVs for urban transportation. Sulaiman said, “the air of Erbil city is poisoned and it’s not suitable for life.”[6]. Although there are various types of LIB have been widely used to power the EVs, the performance characteristics of these batteries are not clearly specified in a more comparable way [7]. According to the literature, the voltage gradient increases the motion of the Li ions by a factor of 100 compared to the concentration gradient [8]. LIB of comparable capacity and voltage are lighter in weight, require less maintenance, and have a higher recharge cycle capacity (number of charge-discharge cycles) compared with traditional lead-acid batteries. The LIB cost 2% less, and its weight was 76% lighter than a sealed lead acid battery of similar capacity [9].

II. EVs

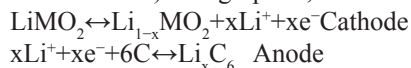
A. EV

Vehicles are with only all-electric driving capability. These use an extremely large battery pack, and can only be recharged with electricity from the grid. These vehicles have zero *in situ* emissions, but they are currently either much more expensive than conventional vehicles or have very limited range. EVs those are contain large lithium-ion battery packs let to provide all of the on board energy [10]. In the near future, EVs including hybrid electric vehicles (HEVs), plug-in hybrid EVs, and pure battery electric vehicles will dominate the clean vehicle market. By 2020, it is expected that more than half of new vehicle sales will likely be EV models. The key and the enabling technology to this revolutionary change is battery. They are required to handle high power (up to a hundred kW) and high energy capacity (up to tens of kWh) within a limited space and weight and at an affordable price [11]. High-voltage LIBs (HVLIBs) are considered as promising devices of energy storage for EV, HEV, and other

high-power equipment. HVLIBs require their own platform voltages to be higher than 4.5 V on a charge [12]. Hitachi sees its automotive LIB business as providing a key pillar in the solution of global environmental problems and intends to contribute in the future through the supply of highly reliable high-performance batteries while also working actively to satisfy future market needs by taking up the challenge of further battery innovation [13]. Micro hybrid vehicles have been introduced into the market to reduce fuel consumption and CO₂-emissions. Some reduction of the pollutions may be achieved through an optimization of the LIBs performance at low temperatures. Another way of increasing its performance would be an increase of its size [14].

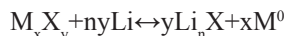
III. ELECTROCHEMICAL REACTIONS

The reaction mechanism of the LIBs involves the migration of Li⁺ cations into (insertion and intercalation) cathode and out of extraction, deintercalation, and anode electrodes. Since Li metal anodes have been largely replaced by graphitic carbon due to safety concerns, the positive electrodes in LIBs act as a source of Li. During discharge, Li⁺ migrates from the anode, through the electrolyte, to the cathode. Concomitantly, an electron is released for every Li⁺ ion involved in the migration to an external circuit where it can power a device and perform work. The half-reactions, or one component of a redox (reduction-oxidation) reaction, of the two electrodes composed of Li metal oxides of the form LiMO₂ (where M is a transition metal) and graphite, can be written as:



In the LiMO₂ case, the transition metal gets oxidized from M³⁺ to M⁴⁺ during charging, with a subsequent reduction from M⁴⁺ to M³⁺ during discharge. Initially, layered LiNiO₂ was considered a promising cathode material considering it is cheaper and less toxic than cobalt.

In the reaction mechanism, Li compounds (lithium sulfide [Li₂S], lithium oxide [Li₂O], and lithium fluoride [LiF]) are formed along with metal nanoparticles during discharging. The overall reaction can be written as:



Where X is either O or F, and M⁰ denotes a transition metal in the metallic state [15].

IV. ELECTROLYTIC SOLUTION AND THE SEPARATOR BETWEEN THE ELECTRODES

Many liquid solvents are available to use as electrolytes, each with a respective viscosity and dielectric constant that can be selected to facilitate the ionic conductivity. Employing a polymer electrolyte imposes further criteria, as electrochemical stability of the backbone and side chains becomes relevant. Typically, ethylene carbonate and dimethyl carbonate are used. In contrast, only a handful of Li salts -Li hexafluorophosphate (LiPF₆), Li triflate (LiSO₃CF₃), Li tetrafluoroborate (LiBF₄), Li perfluoro sulfonimide

(Li⁺[CF₃SO₂NSO₂CF₃]⁻), and among others have been used for the electrolyte. In addition, polyethylene oxide has been the primary focus of polymer electrolytes [15]. When a Li salt is dissolved in an organic mixed solvent, the solution can be used as an electrolyte. The normal electrolytes for LIBs are classified mainly as liquid electrolyte, solid electrolyte, and liquid-solid electrolyte [16]. There are used electrolyte a mixture of organic carbonates such as ethylene carbonate, dimethyl carbonate, and diethyl carbonate containing hexafluorophosphate (LiPF₆) [11]. In this research paper used bamboo carbon fiber BCF@SnO₂@C, the SnO₂ is placed between the BCF template and the coated glucose-derived carbon. According to the research, A high reversible capacity of 627.1 mA h/g is maintained over 100 cycles at a current density of 100 mA/g, showed a huge increase 5 times [17]. Moreover, in another work, there is a new class of carboxylated polyimide (PI) separator (Fig. 1), which can be fabricated through an alkali treatment-based surface modification. The -COOH groups with unshared electron pairs were proposed to contribute to the desolvation of Li-ions and an increase in the Li-ion transport rate. The carboxylated PI separator was conducive to improving the Li-ion transference number. Benefiting from its high Li-ion transference number and slightly increased ionic conductivity, the cell assembled with the carboxylated PI separator achieved a better cycle performance and high rate capability [18].

Chitosan has been applied as a proton-conducting membrane because of its excellent properties. These properties include the following: (i) Biocompatibility, biodegradable polymer, non-toxicity, and abundance in nature, (ii) existence of hydroxyl (OH⁻) and amine (NH³⁺) functional groups, which have lone pair electrons at the chitosan monomer which allow the chelation of a proton (H⁺) donor for battery, and (iii) chemically, thermally, and mechanically stable membrane (stable up to 200°C). By this way, in proton-conducting polymer membranes, proton (H⁺) species are contributed by the addition of salt. Ammonium acetate (NH₄CH₃COO) is one of the salts that doped in proton-conducting polymer membranes. The conductivity of NH₄CH₃COO doped to polyvinyl alcohol resulted in conductivity of approximately 10⁻⁶ S cm⁻¹ achieved a much higher conductivity of 10⁻⁴ S cm⁻¹ when chitosan acetate membrane was complexed with 40 wt.% of NH₄CH₃COO [19]. The other additives for an electrolytic solution are molybdenum trioxide (MoO₃) and phosphorus oxynitride (PON) on the ionic conductivity of the oxide solid electrolyte Li₂O-LiF-P₂O₅. The latter is used for surface modification of the LIBs electrode materials and as the solid electrolyte with higher ionic conductivity for all-solid-state batteries. Furthermore, reported the optimal content of the additives MoO₃ and PON of 1.5 wt% and 10 mol%, respectively, in the structure of the solid electrolyte Li₂O-LiF-P₂O₅ which provides higher ionic conductivity (9.15/10 S/cm and 2.61/10 S/cm, respectively) compared to the solid electrolyte Li₂O-LiF-P₂O₅ without additives (4.4/10 S/cm) at room temperature [20]. There are divide polymer electrolytes into the two large categories of solid

polymer electrolytes and gel polymer electrolytes (Fig. 2). The solid polymer electrolyte systems were including dry solid polymer electrolytes, polymer-in-salt systems (rubbery electrolytes), and single-ion conducting polymer electrolytes. Solid polymer electrolytes had poor ionic conductivity, which is lower than 10^{-5} S/cm [21].

Furthermore, there is report on using red phosphorus's large theoretical charge capacity, which is roughly 7 times as high as graphite's. Blending phosphorus with carbon, which is a common approach, improves conductivity but dilutes the phosphorus, limiting the boost in charge capacity. Hence, Tuan's group formed iodine doped red phosphorus nanoparticles by reacting PI_3 with ethylene glycol and cetyltrimethylammonium bromide [22].

According to the functionalization of ether groups, others are used mainly as electrolyte, additive, binder, separator or anode in LIBs. When functionalized cation ionic liquids were used as the electrolyte, ether-based ionic liquids had better properties for LIBs, but it was very difficult to gain pure ionic liquids. Ether-based polymers could be used as electrolyte and separator [16]. Yang's group reported that ether functionalized quaternary ammonium cation ionic liquids (1 and 2 from Scheme 1) could be used as electrolytes for LIB. When the quaternary ammonium cation ionic liquids were used as electrolytes in Li/LiFePO₄ batteries, these batteries showed good cycling properties. Consequently, electrolytes with two ether groups had better rate properties than those with one ether group. This means that ionic liquids with low melting points were good for use in LIBs. According to the research, the rate-determining process for Li⁺ migration achieved under such low temperatures, so that

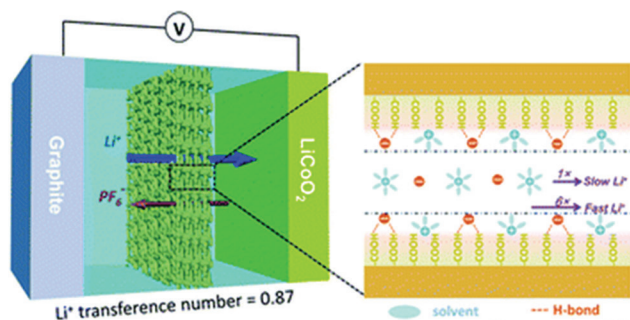


Fig. 1. Carboxylate polyimide separator between anode and cathode electrodes.

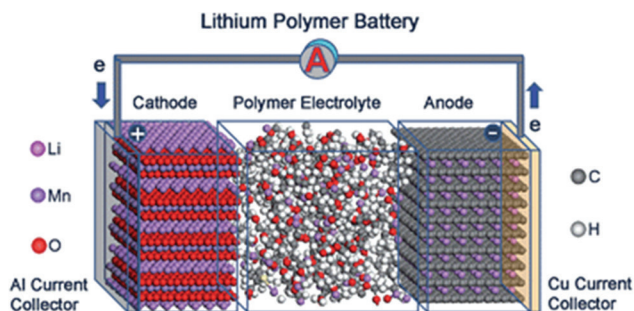


Fig. 2. A polymer electrolyte between the two electrodes [21].

an optimum electrolyte formulation could be designed to maximize the energy output (Fig. 3) [16].

V. ELECTRODES

The electrodes composition in LIBs is a source for Li ions to transfer from one to another through cycling and charging of the cell. For designing electrodes with improved lifetime and electromechanical efficiency, it is crucial to understand how diffusion evolved over consecutive charging-recharging cycles [23]. The electrodes under current development are from anodes: Carbonaceous electrodes, silicon, tin, and $Li_4Ti_5O_{12}$; from layered cathodes: $LiCoO_2$, Li-rich, and $LiNi_yMn_yCo_{1-2y}O_2$ (LNMCO); from spinel: $LiMn_2O_4$, and from olivine: $LiFePO_4$ are selected. These materials raise the performance of the LIB [24]. Another material of an electrode fabricated using a composite containing less crystalline melt quenched vanadium oxide embedded on graphene oxides 50% (MVG050) in LIB. The reversible Li cycling properties of MVGO50 are evaluated by galvanostatic charge-discharge cycling studies. MVGO50 electrodes exhibited rate capacity to 200 mA h/g at a current of 0.1 C rate and remained stable during cycling [17]. There was reported an advanced LIB based on a graphene ink anode and a Li iron phosphate (LFP) cathode. By carefully balancing the cell composition and suppressing the initial irreversible capacity of the anode in the round of few cycles, and demonstrated an optimal battery performance in terms of specific capacity [25].

VI. CATHODE ELECTRODES COMPOSITIONS

There was developed a novel poly-(1,4-anthraquinone)/carbon nanotube (P14AQ/CNT) nanocomposite through a simple *in situ* polymerization, to improve the rate performance of the LIB. As reported that the CNT were homogeneously distributed in the composite. CNT utilized as the cathode material for LIB; the P14AQ/CNT composite exhibits excellent cycling stability with a specific capacity [26]. With respect to the literature, the Li metal silicates (Li_2MSiO_4) (where M = Mn, Fe, and Co) have a great potential in rechargeable LIBs as poly-anion cathodes [27].

Single-phase $Na_{1.2}V_3O_8$ materials with single and hierarchical nanobelt morphologies are prepared. The products obtained are employed as cathode materials for



Scheme 1. The structures of quaternary ammonium cation ionic liquids.

LIBs. Their electrochemical activities are demonstrated through galvanostatic cycling and cyclic voltammetry. It serves as channels for facile Li diffusion are capable of exhibiting higher maximum capacities of approximately 218 mA h/g compared to hierarchical nanobelts with a maximum capacity of approximately 197 mA h/g versus Li/Li⁺ at a current density of 200 mA/g [28]. According to the literature, a material and processing platform that realizes high-performance nanostructured Li manganese oxide spinel cathodes with conformal graphene coatings as a conductive additive. The resulting nanostructured composite cathodes concurrently raise the capacity and cyclic stability [29].

For the cathode, there are three choices: Layered LiMO₂ (M = Mn, Co, and Ni), spinel LiMn₂O₄, and olivine LiFePO₄ (Fig. 4). Each of these three cathodes had their advantages and disadvantages. The layered structure gives the highest practical capacity (currently up to 180 A h/kg) among the three, but suffers from structural and/or chemical instabilities during cycling depending on the chemical composition and state of charge (Li content in the electrode) because of migration the transition-metal ions from the octahedral sites of the transition metal layer to the octahedral sites of the Li layer through a neighboring tetrahedral site [30].

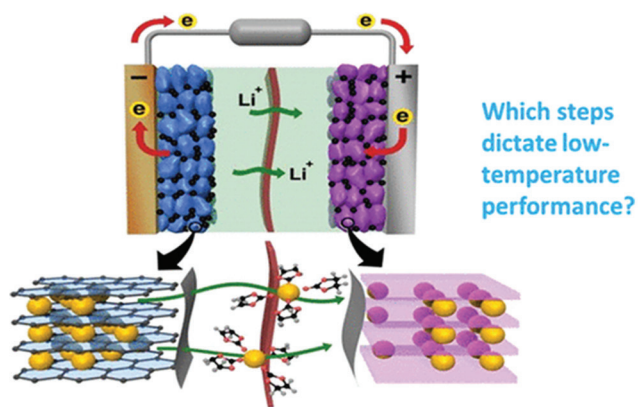


Fig. 3. Migration of lithium-ion through the membrane [16].

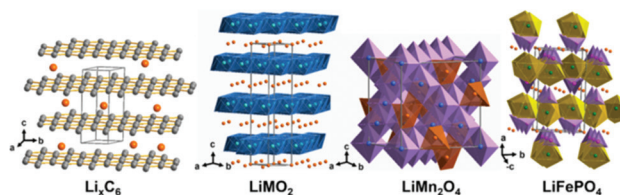


Fig. 4. Crystal structures of the cathode electrode [30].

VII. ANODE ELECTRODE COMPOSITIONS

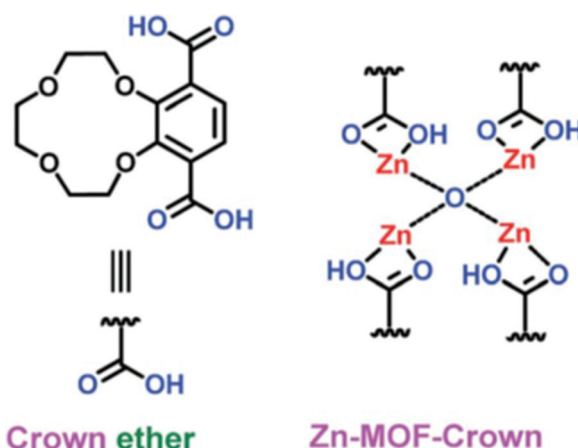
For anode side, it focused on materials which can host Li either by alloying or by a conversion mechanism. However, a new class of potential next-generation anodes is gaining continuously increasing attention: Conversion/alloying materials. It is possible approaches to realize a combined conversion and alloying mechanism in a single compound, starting either from pure conversion or pure alloying materials (Fig. 5) [31].

According to the literature, crown ether compared with cation ionic liquids and polymers, crown ether was easier to synthesize, and crown ether-based metal-organic frameworks (MOFs) had better charge capacity with excellent cycling performance. It will be significant to synthesize novel crown ether-based materials, which could be utilized to construct the anode for LIBs, sodium ion batteries, and magnesium ion batteries. The compound used by Zhao's group was a microporous Zn-based MOF containing 12-crown-4 units (Zn-MOF-Crown) (as shown in Scheme 2) as the anode material in the LIB, with a charge capacity of 273 mA h/g. The MOF structure integrity never was damaged because of the interaction between the Li⁺ ions and crown ether. The Zn-MOF-Crown completed with Li⁺ ions and Li⁺@Zn-MOF-Crown was formed with a charge capacity of 348 mA h/g and long-term cycling ability. By this way, the introduction of crown ether could improve the performance in green energy systems [16].

As reported, the produced crystalline PSi coated with carbon layers shows excellent electrochemical performance when served as LIB anodes. The reversible specific capacity is about 2250 mA h/g at 0.1 A/g and the capacity reached to 90% after cycling at high current density of 2 A/g for 320 cycles. It was a way for the massive production of



Fig. 5. Alloying and conversion for anode electrode.



Scheme 2. The structure of Zn-metal-organic frameworks-crown.

porous Si as high-performance anodes in LIB industry [32]. In other work, single (Co_3O_4), binary ($\text{Co}_3\text{O}_4/\text{ZnO}$), and ternary ($\text{Co}_3\text{O}_4/\text{ZnO}/\text{NiO}$) nanomaterials were successfully synthesized by Pechini method followed by a calcination step. High capacity retention and lowest voltage hysteresis were achieved with the ternary material. This was a positive impact of multiple element strategies on the cycle life of anode materials [33]. The hydrogenated graphene showed significant improvement in battery performance compared with as-prepared graphene. For minor modifications to graphene can dramatically improve electrochemical performance in both LIBs and sodium-ion batteries [34]. Furthermore, for anode electrode used tin oxide (SnO_2) based material is regarded as a promising anode candidate due to its high theoretical reversible Li^+ storage capacity (782 mA h/g), low cost, and facile synthesis technology [35].

According to the density, functional theory calculations studied (as reported in the reference) on the Li ion storage capacity using of biphenylene membrane and phagraphene which are two-dimensional defected-graphene-like membranes. Both membranes show a larger capacity than graphene, Li_2C_6 and $\text{Li}_{1.5}\text{C}_6$ compared to LiC_6 . They found that Li is very mobile on these materials and does not interact as strongly with the membranes. Their inventions indicated that both membranes are suitable materials for LIB anodes [36].

VIII. LI-ION BATTERY PERFORMANCE

To improve battery performance, it is important to characterize and quantify real electrode microstructures in three dimensions, and understand how these structures affect performance and cycle life. Porous carbon electrodes play an important role in both battery and fuel cell operation, where parameters such as porosity, tortuosity, and pore-size distribution determine the transport properties of the electrode, as well as the kinetics of the electrochemical reactions. These properties play key roles in determining the performance of battery electrodes. LFP LiFePO_4 is a commercially available electrode material for LIBs for EVs and energy storage applications. There are many advantages of this material, which include excellent cycle life (Table I) and high intrinsic safety. The author's enhancement for 3D imaging, including novel advanced quantification, on a commercial LFP LiFePO_4 cathode [37].

The large radius of Na^+ (0.98 Å), much larger than that of Li^+ (0.69 Å), determines that Na-ion is difficult to insert into the crystal structure of host materials commonly used for LIBs. The extraordinary electrochemical performance promises the N-doped porous carbon networks an application in LIBs, Na-ion battery, and Zn-air battery. The synthesized N-doped porous carbon networks display a high specific capacity of 1534 mA h/g versus Li/Li^+ and 335 mA h/g versus Na/Na^+ at current density 100 mA/g, with remarkable cycling stability and good rate performance [38].

The spinels $\text{LiMn}_{1.5}\text{Me}_{0.5}\text{O}_4$ and LiMnMeO_4 (Me: Ni, Fe) were prepared using either a sol-gel process in the case of nickel doping or a solid-state reaction in the case of iron

doping. The material $\text{LiMn}_{1.5}\text{Ni}_{0.5}\text{O}_4$ could intercalate both chemically and electrochemically second Li at 3 V without structural changes and with a large discharge capacity of 160 mA/h/g. This material at 4.7 V plateau was 90 mA/h/g capacity due to the oxidation of divalent nickel to the tetravalent state when first charged [39]. From other work used Li nickel manganese spinel $\text{LiNi}_{0.5}\text{Mn}_{1.5}\text{O}_4$ (LNMO) cathode is the most promising candidate among the 5 V cathode materials for HVLIBs due to its flat plateau at 4.7 V. The degradation of cyclic performance is very serious when LNMO cathode operates over 4.2 V [12].

N-Doped-carbon-coated 2–4 nm SnO_2 nanoparticles were synthesized through a facile MOF coating process followed by calcination of the $\text{SnO}_2@\text{MOF}$ composite. This material has advantages of a synergistic effect of SnO_2 nanoparticles and carbon structure; these materials exhibit excellent electrochemical performance. The reversible specific capacity of 1032 mA h g^{-1} was maintained at 100 mA/g after 150 cycles with a coulombic efficiency of 99%. When the current was increased to 500 mA/g, a capacity of 600 mA h/g was attained. In the first cathodic sweep process, there were decomposition of SnO_2 to form Sn and the formation of solid electrolyte interphase. Then, there formed of Li–Sn alloy. As from Zhang group research, SnO_2 reduced to Sn and Li_2O . In the anodic sweep process, there was formed of Li_xSn alloy through Li alloying with tin and Li_xSn alloy and Li_2O transforming into SnO_2 . The electrochemical reaction mechanism of Li with SnO_2 in LIBs can be described in the following equations:

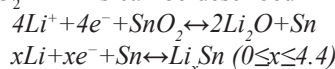


TABLE I
EFFECT OF COMPOSITION AND STABILITY ON CAPABILITY FOR LITHIUM-ION BATTERY

Compound	Current (mA h/g)	Cycle (C)	References
MnO@N-C/rGO	864.7	70	[40]
MnO@N-C/rGO	2000	1300	[40]
SnO_2 nanoparticles	1032	150	[40]
$\text{LiMn}_{1.5}\text{Ni}_{0.5}\text{O}_4$	160	3	[12]
$\text{Co}_3\text{O}_4/\text{ZnO}/\text{NiO}$	649	1	[33]
Hydrogenated graphene	488	50	[34]
Hydrogenated graphene	491	20	[34]
Crystalline PSi	2250	320	[32]
Zn-MOF-Crown	348	Long-term cycling	[16]
$\text{Na}_{1.2}\text{V}_3\text{O}_8$	207 and 173	100	[28]
P14AQ/CNT	233	100	[26]
P14AQ/CNT	165	5	[26]
MVGO50	200	0.1	[17]
BCF@ $\text{SnO}_2@\text{C}$	627.1	over 100	[17]
LiFePO_4	180	3	[30]
N-doped porous carbon networks	335	Cycling stability	[38]
Carbon (natural bamboo waste)	1160	0.1	[24]
Carbon (natural bamboo waste)	710	0.2	[24]
Carbon (natural bamboo waste)	695	0.5	[24]
Carbon (natural bamboo waste)	580	1	[24]

On the other hand, the charge transfer resistance (the diameter of the semicircle) decreased after 100th cycling, indicating the first several cycles are the electrode activation process and decrease the impedance value of SnO₂@C electrode, which it was a significant improvement in the rate performance and kinetics of the reaction on cycling. In comparison with other SnO₂-based anode materials for LIBs, the synergistic effect of the 2–4 nm SnO₂ nanoparticles after calcination and the porous nitrogenous carbon structure allow our materials presents the high electrochemical performance [40].

The MnO material used as a LIB anode associated with the pulverization and gradual aggregation during the conversion process. Such dual carbon protection endows MnO@N-C/rGO with excellent structural stability and enhanced charge transfer kinetics. MnO@N-C/rGO shows outstanding reversible capacity, cyclability (Table I), and rate capability, from the smart function of the dual carbon, mesoporous structure, and N-doping effect [40].

According to the literature, the compound LiMn_{1.5}Ni_{0.5}O₄ can intercalate the second Li both chemically and electrochemically, leading to the formation of a new Li₂Mn_{1.5}Ni_{0.5}O₄ material with the same cubic spinel structure. This material had only one plateau at around 3 V versus Li/Li⁺ with a large discharge capacity of 160 mAh/g and fairly good cyclability [41].

There was reported as prepared a cylindrical LIBs of LiNi_{0.8}Co_{0.15}Al_{0.05}O₂ (LNCAO) (Fig. 6) prepared with graphite. The electrochemical reactivity of the LNCAO derivatives with rock-salt domains was examined in non-aqueous Li cells, and it was found that the rechargeable capacities decreased as the amount of rock-salt domain increased. A relation is remarkable in the Li insertion direction into the structure, which is ascribed to slow Li ion mobility due to nickel ions in the Li layers [42].

IX. CHARGING AND DISCHARGING

The success of EVs will be highly dependent on whether charging stations can be built for easy access. This is also critical for the potential grid supports that EVs can provide.

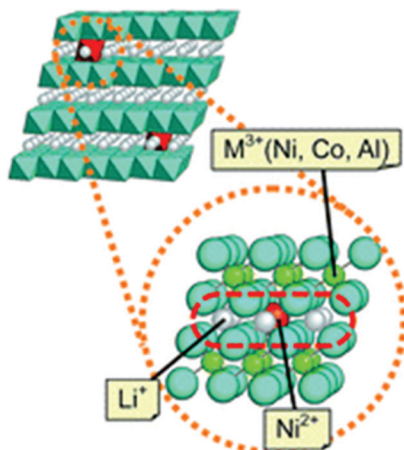
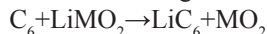


Fig. 6. The structure and composition (LNCAO) of cylindrical lithium-ion batteries.

The first place considered for charging stations should be homes and workplaces. Other potential locations with high populations include gas stations, shopping centers, and so on. Precisely, during charging, Li ions, driven by the potential difference supplied by the charging unit, intercalate into the interlayer region of graphite. The arrangement of Li⁺ in graphite is coordinated by the surface–electrolyte–interface layer, which is formed during the initial activation process. The active material in the positive electrode is a Li-containing metal oxide, during charging, the Li⁺ hops onto the surface, moves through the electrolyte, and finally arrives at the negative electrode. The oxidation state of the host metal will increase and return electrons to the outside circuitry. During discharge, the process is reversed. Li-ions now move from the intercalation sites in the negative electrode to the electrolyte and then to the original site in the LiMO₂ crystal (Fig. 7) [11].



A battery charge equalization controller is capable to enhance the battery's performance, life cycle, and safety. A charge equalization algorithm is proposed and implemented using a battery monitoring integrated circuit for monitoring and equalization of an 8-cell battery pack using bidirectional flyback DC-DC converter as the channel for charging and discharging of the battery cell. The proposed equalization method proves an effective and automated system to modularize the battery charge that improves the safety and life cycle of the battery. The cell switch allows a specific cell to be connected through flyback DC-DC converter (Fig. 8) to cell pack for discharging or charging based on the cell as overcharged or undercharged, respectively [2].

Charging the LNMO at high voltage (5 V) is proposed to be beneficial for its reversible capacity; however, it will accelerate the performance degradation. Charging the LIBs at high voltage can accelerate the oxidation of the electrolyte and result in the formation of a high impedance film on the electrodes surface. Furthermore, the formation of hydrofluoric acid at high voltage leads to a severe deterioration of the cycling performance. The electrolyte reactions also result in gaseous products at higher potentials, which will cause pouch and prismatic cells to bulge. Therefore, gas production is another failure mechanism that

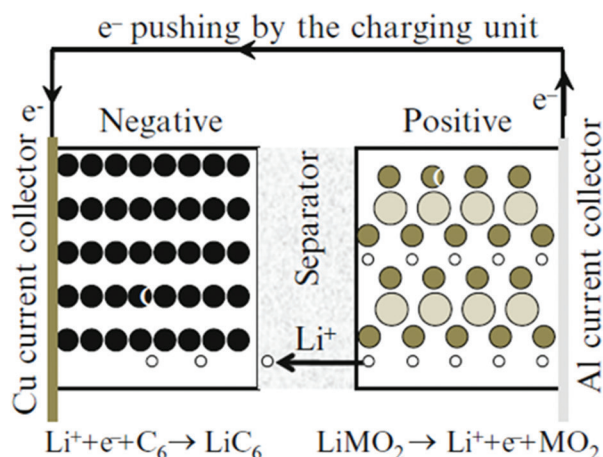


Fig. 7. Schematic of the charging operation of a Li-ion battery.

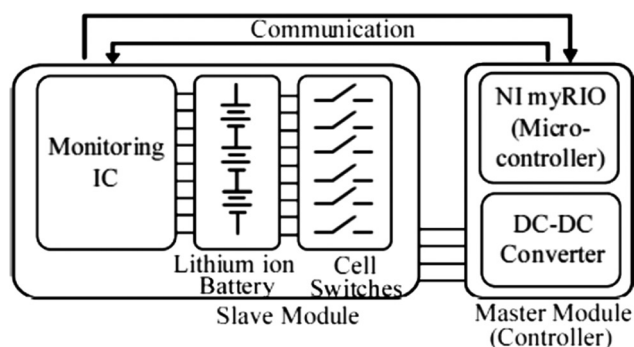


Fig. 8. Equalization control system block diagram [2].

often occurs in Li-ion cells at high voltage. In general, these gassing reactions can be attributed to electrolyte reactions on electrodes, and the gas products are H_2 , CO_2 , and low-weight hydrocarbons [12]. In this paper, remaining discharge energy estimation is proposed using the recursive least square-unscented Kalman filter. The recursive least square is applied to identify the parameters of the battery pack model online. The unscented Kalman filter is employed in battery pack remaining discharge energy and energy utilization ratio estimation. The experimental results estimate that the battery pack remaining discharge energy with high accuracy [43]. After 100 cycles, the resistance of the cell is larger than that after the first cycle, which may be resulted from the dissolution of part long chain Li poly-sulfides during both discharge and charge processes, reducing the migration speed of Li-ions in the electrolyte [24]. LIBs are easily overheated during discharge/charge operations with large current output/input [44]. Hence, heat is produced locally by undesired chemical reactions [45]. Furthermore, the thermal runaway follows a mechanism of chain reactions, during which the decomposition reaction of the battery component materials occurs one after another [46]. Temperature uniformity of a heated LIB cell is acceptable by decreasing heating power and thickness of a LIB cell if there is no safety problem on the structure [47]. The findings revealed that the battery charge capacity decay rate tends to increase with aging of the batteries due to problems that can be attributed to retarded electrode functionalities, Li corrosion, and reduced reaction surface area, which impairs the functionalities of the electrodes and the electrolytes and impedes Li-ion diffusion through the electrolytes [48]. On the other hand, there are so much valued metals in the spent LIBs, such as Co, Li, and Mn. Therefore, recycling of these spent batteries is necessary and important from both economical aspect and environmental protection [49]. MOFs are a class of typical porous materials construction by metal ions and polyfunctional organic ligands. Moreover, MOFs are regarded as ideal self-sacrificial precursors/templates to develop highly porous functional materials, which are suitable for multiple applications such as photocatalysis, batteries, and supercapacitors [50].

X. CONCLUSIONS

LIB has a good life cycle, easier maintenance, and environmentally friendly compared with other types of

batteries. The LIB has been extensively applied as the only power of pure EVs because of its high energy density, long lifespan, and low self-discharging. The success of EVs will be highly dependent on whether charging stations can be built for easy access. There is a clear need to incorporate uncertainties in battery charge capacity decay modelling to enhance the robustness of prognostic estimates of remaining useful life in the future for mission-critical applications. Furthermore, further optimization of the dimensioning of the battery compositions is consequently an important body of future work.

REFERENCES

- [1] D. Di Lecce, R. Verrelli and J. Hassoun, "Lithium-ion batteries for sustainable energy storage: Recent advances towards new cell configurations," *Green Chemistry*, vol. 19, no. 15, pp. 3442-3467, 2017.
- [2] M. A. Hannan, M. M. Hoque, S. E. Peng and M. N. Uddin, "Lithium-ion battery charge equalization algorithm for electric vehicle applications," *IEEE Transactions on Industry Applications*, vol. 53, no. 3, pp. 2541-2549, 2017.
- [3] J. P. Meulhose and R. Zhao, *A Comparative Study of Lithium - Ion Batteries*, California: University of South California, p. 31, 2010.
- [4] P. Patel, "Improving the lithium-ion battery," *ACS Scent Science*, vol. 4, pp. 161-162, 2015.
- [5] N. S. Mubenga, Z. Linkous and T. Stuart, "A bilevel equalizer for large lithium ion batteries," *Batteries*, vol. 3, no. 4, p. 39, 2017.
- [6] S. G. Muhammad, 'Poison Gases' *Lagal Ranj Interview*, Erbil, Iraq: Rudaw, Television, 2015.
- [7] X. Chen, W. Shen, T. T. Vo, Z. Cao and A. Kapoor, "An Overview of Lithium-Ion Batteries for Electric Vehicles," in *IPEC, 2012 Conference on Power and Energy, IEEE*, pp. 230-235, 2012.
- [8] J. Summerfield, "Modeling the lithium ion battery," *Journal of Chemical Education*, vol. 90, no. 4, pp. 453-455, 2013.
- [9] E. E. Hockersmith, B. Gabriel, D. D. Nathan and S. Achord, "A lightweight battery for backpack electrofishing," *North American Journal of Fisheries Management*, vol. 33, no. 2, pp. 265-268, 2013.
- [10] N. Xue, "Design and Optimization of Lithium-ion Batteries for Electric-Vehicle Applications," Citeseer, 2014.
- [11] K. Young, C. Wang, L. Y. Wang and K. Strunz, "Electric vehicle battery technologies," in *Electric Vehicle Integration into Modern Power Networks*, New York: Springer, pp. 15-56, 2013.
- [12] X. Xu, S. X. Deng, H. Wang, J. B. Liu and H. Yan, "Research progress in improving the cycling stability of high-voltage LiNiO. 5Mn1. 5O4 cathode in lithium-ion battery," *Nano-Micro Letters*, vol. 9, no. 2, p. 22, 2017.
- [13] K. Higashimoto, H. Homma, Y. Uemura, H. Kawai, S. Saibara and K. Hironaka, "Automotive lithium-ion batteries," *Hitachi Review*, vol. 60, no. 1, p. 17, 2011.
- [14] M. K. Matthias Kuipers and D. U. Sauer, "Critical analysis of hybrid battery systems for micro hybrid vehicles based on the parallel combination of a lead acid-and-a lithium ion battery," Jülich Aachen Research Alliance, no. Conference Paper, p. 14, 2016.
- [15] P. J. Sideris and S. G. Greenbaum, "Lithium ion batteries, electrochemical reactions," in *Batteries for Sustainability*, New York: Springer, pp. 239-283, 2013.
- [16] Q. Li, D. Lu, J. Zheng, S. Jiao, L. Luo, C. M. Wang, K. Xu, J. G. Zhang and W. Xu, "Li+-desolvation dictating lithium-ion battery's low-temperature performances," *ACS Applied Materials and Interfaces*, vol. 9, no. 49, pp. 42761-42768, 2017.
- [17] M. Sreejesh and K. S. Sulakshana Shenoy, D. Kufian, A. K. Arof, H. S. Nagaraja, "Melt quenched vanadium oxide embedded in graphene oxide sheets as composite electrodes for amperometric dopamine sensing and lithium ion battery

- applications," *Applied Surface Science*, vol. 410, pp. 336-343, Jul. 15, 2017.
- [18] C. E. Lin, H. Zhang, Y. Z. Song, Y. Zhang, J. J. Yuan and B. K. Zhu, "Carboxylated polyimide separator with excellent lithium ion transport properties for a high-power density lithium-ion battery," *Journal of Materials Chemistry A*, vol. 6, no. 3, pp. 991-998, 2018.
- [19] S. S. Alias, S. M. Chee and A. A. Mohamad, "Chitosan-ammonium acetate-ethylene carbonate membrane for proton batteries," *Arabian Journal of Chemistry*, vol. 10, pp. S3687-S3698, 2017.
- [20] A. Tron, A. Nosenko, Y. D. Park and J. Mun, "Enhanced ionic conductivity of the solid electrolyte for lithium-ion batteries," *Journal of Solid State Chemistry*, vol. 258, pp. 467-470, 2018.
- [21] L. Long, S. Wang, M. Xiao and Y. Meng, "Polymer electrolytes for lithium polymer batteries," *Journal of Materials Chemistry A*, vol. 4, no. 26, pp. 10038-10069, 2016.
- [22] M. Jacoby, "Phosphorus boosts lithium-ion battery charge capacity," *Chemical and Engineering News*, vol. 95, no. 5, pp. 8-8, 2017.
- [23] M. Peigney, "Cyclic steady states in diffusion-induced plasticity with applications to lithium-ion batteries," *Journal of the Mechanics and Physics of Solids*, vol. 111, pp. 530-556, 2018.
- [24] Y. Cheng, S. Ji, Y. Liu and J. Liu, "High sulfur loading in activated bamboo-derived porous carbon as a superior cathode for rechargeable Li-S batteries," *Arabian Journal of Chemistry*, vol. 11, pp. 739-754, 2015.
- [25] J. Hassoun, F. Bonaccorso, M. Agostini, M. Angelucci, M. G. Betti, R. Cingolani, M. Gemmi, C. Mariani, S. Panero, V. Pellegrini and B. Scrosati, "An advanced lithium-ion battery based on a graphene anode and a lithium iron phosphate cathode," *Nano Letters*, vol. 14, no. 8, pp. 4901-4906, 2014.
- [26] D. Tang, W. Zhang, Z. A. Qiao, Y. Liu and D. Wang, "Polyanthraquinone/CNT nanocomposites as cathodes for rechargeable lithium ion batteries," *Materials Letters*, vol. 214, pp. 107-110, 2018.
- [27] K. Huang, B. Li, M. Zhao, J. Qiu, H. Xue and H. Pang, "Synthesis of lithium metal silicates for lithium ion batteries," *Chinese Chemical Letters*, vol. 28, no. 12, pp. 2195-2206, 2017.
- [28] Y. W. Ko, S. S. Pramana and M. Srinivasan, "Electrospun single-phase Na_{1.2}V₃O₈ materials with tunable morphologies as cathodes for rechargeable lithium-ion batteries," *ChemElectroChem*, vol. 2, no. 6, pp. 837-846, 2015.
- [29] K. S. Chen, R. Xu, N. S. Luu, E. B. Secor, K. Hamamoto, Q. Li, S. Kim, V. K. Sangwan, I. Balla and L. M. Guiney, "Comprehensive enhancement of nanostructured lithium-ion battery cathode materials via conformal graphene dispersion," *Nano Letters*, vol. 17, no. 4, pp. 2539-2546, 2017.
- [30] A. Manthiram, "An outlook on lithium ion battery technology," *ACS Central Science*, vol. 3, no. 10, pp. 1063-1069, 2017.
- [31] D. Bresser, S. Passerini and B. Scrosati, "Leveraging valuable synergies by combining alloying and conversion for lithium-ion anodes," *Energy and Environmental Science*, vol. 9, no. 11, pp. 3348-3367, 2016.
- [32] L. Sun, F. Wang, T. Su and H. Du, "Room-temperature solution synthesis of Mesoporous silicon for lithium ion battery anodes," *ACS Applied Materials and Interfaces*, vol. 9, no. 46, pp. 40386-40393, 2017.
- [33] T. G. U. Ghobadi, M. Kunduraci and E. Yilmaz, "Improved lithium-ion battery anode performance via multiple element approach," *Journal of Alloys and Compounds*, vol. 730, pp. 96-102, 2018.
- [34] J. C. Pramudita, D. Pontiroli and G. Magnani, "Graphene and selected derivatives as negative electrodes in sodium- and lithium-ion batteries," *ChemElectroChem*, vol. 2, no. 4, pp. 600-610, 2015.
- [35] M. S. Wang, Z. Q. Wang, Z. L. Yang, Y. Huang, J. Zheng and X. Li, "Carbon nanotube-graphene nanosheet conductive framework supported SnO₂ aerogel as a high performance anode for lithium ion battery," *Electrochimica Acta*, vol. 240, pp. 7-15, 2017.
- [36] D. Ferguson, D. J. Searles and M. Hankel, "Biphenylene and phagraphene as lithium ion battery anode materials," *ACS Applied Materials and Interfaces*, vol. 9, no. 24, pp. 20577-20584, 2017.
- [37] V. Y. M. Biton, F. Tariq, M. Kishimoto and N. Brandon, "Enhanced imaging of lithium ion battery electrode materials," *Journal of The Electrochemical Society*, vol. 164, no. 1, pp. A6032-A6038, 2017.
- [38] L. Wang, C. Yang, S. Dou, S. Wang, J. Zhang, X. Gao, J. Maa and Y. Yu, "Nitrogen-doped hierarchically porous carbon networks: Synthesis and applications in lithium-ion battery, sodium-ion battery and zinc-air battery," *Electrochimica Acta*, vol. 219, pp. 592-603, 2016.
- [39] K. Amine, H. Tukamoto, H. Yasuda and Y. Fujita, "Preparation and electrochemical investigation of LiMn₂-xM_xO₄ (M: Ni, Fe, and x = 0.5, 1) cathode materials for secondary lithium batteries," *Journal of Power Sources*, vol. 68, no. 2, pp. 604-608, 1997.
- [40] W. Zhang, J. N. Li, J. Zhang, J. Z. Sheng, T. He, M. Y. Tian, Y. F. Zhao, C. J. Xie, L. Q. Mai and S. C. Mu, "Top-down strategy to synthesize mesoporous dual carbon armored MnO nanoparticles for lithium-ion battery anodes," *ACS Applied Materials and Interfaces*, vol. 9, no. 14, pp. 12680-12686, 2017.
- [41] M. Winter, J. O. Besenhard, M. E. Spahr and P. Novák, "Insertion electrode materials for rechargeable lithium batteries," *Advanced Materials*, vol. 10, no. 10, pp. 725-763, 1998.
- [42] Y. Makimura, T. Sasaki, T. Nonaka, Y. F. Nishimura, T. Uyama and C. Okuda, "Factors affecting cycling life of LiNi_{0.8}Co_{0.15}Al_{0.05}O₂ for lithium-ion batteries," *Journal of Materials Chemistry A*, vol. 4, no. 21, pp. 8350-8358, 2016.
- [43] X. Zhang, Y. Wang, C. Liu and Z. Chen, "A novel approach of remaining discharge energy prediction for large format lithium-ion battery pack," *Journal of Power Sources*, vol. 343, pp. 216-225, 2017.
- [44] T. Dong, P. Peng and F. Jiang, "Numerical modeling and analysis of the thermal behavior of NCM lithium-ion batteries subjected to very high C-rate discharge/charge operations," *International Journal of Heat and Mass Transfer*, vol. 117, pp. 261-272, 2018.
- [45] A. Nyman and H. Ekström, "Modeling the lithium-ion battery," *IEEE Spectrum: Technology and Science*, vol. pp. 3, 2012.
- [46] X. Feng, M. Ouyang, X. Liu, L. Lu, Y. Xia and X. He, "Thermal runaway mechanism of lithium ion battery for electric vehicles: A review," *Energy Storage Materials*, vol. 10, pp. 246-267, 2018.
- [47] Z. Lei, Y. Zhang and X. Lei, "Temperature uniformity of a heated lithium-ion battery cell in cold climate," *Applied Thermal Engineering*, vol. 129, pp. 148-154, 2018.
- [48] C. I. Ossai and N. Raghavan, "Statistical characterization of the state-of-health of lithium-ion batteries with weibull distribution function - A consideration of random effect model in charge capacity decay estimation," *Batteries*, vol. 3, no. 4, p. 32, 2017.
- [49] A. Nayl, R. Elkhshab, S. M. Badawy and M. El-Khateeb, "Acid leaching of mixed spent Li-ion batteries," *Arabian Journal of Chemistry*, vol. 10, pp. S3632-S3639, 2017.
- [50] J. Huang, G. Fang, K. Liu, J. Zhou, X. Tang, K. Cai and S. Liang, "Controllable synthesis of highly uniform cuboid-shape MOFs and their derivatives for lithium-ion battery and photocatalysis applications," *Chemical Engineering Journal*, vol. 322, pp. 281-292, 2017.